

8-1-2008

Zn- and O-Face Polarity Effects at ZnO Surfaces and Metal Interfaces

Yufeng Dong

Z-Q. Fang

David C. Look

Wright State University - Main Campus, david.look@wright.edu

G. Cantwell

J. Zhang

See next page for additional authors

Follow this and additional works at: <https://corescholar.libraries.wright.edu/physics>



Part of the [Physics Commons](#)

Repository Citation

Dong, Y., Fang, Z., Look, D. C., Cantwell, G., Zhang, J., Song, J. J., & Brillson, L. J. (2008). Zn- and O-Face Polarity Effects at ZnO Surfaces and Metal Interfaces. *Applied Physics Letters*, 93 (7), 72111. <https://corescholar.libraries.wright.edu/physics/96>

This Article is brought to you for free and open access by the Physics at CORE Scholar. It has been accepted for inclusion in Physics Faculty Publications by an authorized administrator of CORE Scholar. For more information, please contact library-corescholar@wright.edu.

Authors

Yufeng Dong, Z-Q. Fang, David C. Look, G. Cantwell, J. Zhang, J. J. Song, and L. J. Brillson

Zn- and O-face polarity effects at ZnO surfaces and metal interfaces

Yufeng Dong,^{1,a)} Z-Q. Fang,² D. C. Look,² G. Cantwell,³ J. Zhang,³ J. J. Song,³ and L. J. Brillson^{1,4}

¹Department of Electrical and Computer Engineering, The Ohio State University, Columbus, Ohio 43210, USA

²Semiconductor Research Center, Wright State University, Dayton, Ohio 45435, USA

³ZN Technology Inc., 910 Columbia St., Brea, California 92821, USA

⁴Department of Physics and Center for Materials Research, The Ohio State University, Columbus, Ohio 43210, USA

(Received 30 July 2008; accepted 31 July 2008; published online 22 August 2008)

Depth-resolved cathodoluminescence spectroscopy, current-voltage, capacitance-voltage, and deep level transient spectroscopy of ZnO (0001) Zn- and (000 $\bar{1}$) O-polar surfaces and metal interfaces show systematically higher Zn-face near band edge emission and lower near-surface defect emission. Even with remote plasma decreases of the 2.5 eV near-surface defect emission, (0001)-Zn face emission quality still exceeds that of (000 $\bar{1}$)-O face. Ultrahigh vacuum-deposited Au and Pd diodes on as-received and O₂/He plasma-cleaned surfaces display a strong polarity dependence that correlates with defect emissions, traps, and interface chemistry. A comprehensive model accounts for the polarity-dependent transport properties and their correlations with carrier concentration profiles. © 2008 American Institute of Physics. [DOI: 10.1063/1.2974983]

ZnO stands out as one of the most important candidates for next generation opto- and microelectronics.¹ Metal/ZnO interfaces are essential to all ZnO electronic device applications, yet fabricating high quality and thermally stable rectifying and Ohmic ZnO contacts remains a challenge and their electronic properties have only recently been explored in detail.²⁻⁷ Metals on semiconductors seldom obey the Schottky–Mott theory, i.e., their Schottky barrier heights are not proportional to their work functions.⁸ Previous ZnO surface studies revealed the importance of surface adsorbates, near-interface native defects, and thermally induced interface chemical interactions at metal/ZnO contacts.^{3,9,10} Stabilization mechanisms of Zn(0001)- or O(000 $\bar{1}$)-terminated faces are still controversial, yet few experimental studies compare them.¹¹ Differences between hydrothermal ZnO polar surfaces were ascribed to surface band bending induced by spontaneous polarization,¹² while melt-grown ZnO exhibits only a small difference in band bending.¹³ It is still not clear which polar face should give better Schottky contacts because few comparisons between two polarities exist regarding their surface optical properties, defect concentrations, metal reactivities with various metal contacts, and Schottky barrier heights.

We used nanoscale depth-resolved cathodoluminescence spectroscopy (DRCLS) coupled with surface science and electronic transport techniques to probe the polarity-dependent properties of (0001) Zn- and (000 $\bar{1}$) O-polar surfaces of low bulk defect ZnO crystals and their metal contacts. DRCLS, remote O₂/He plasma (ROP) processing and deep level transient spectroscopy (DLTS) are described elsewhere.^{3,14} Single crystal ZnO samples grown by vapor-phase process at ZN Technology Inc. and polished chemo-mechanically on both the (0001) and (000 $\bar{1}$) faces had

mid-10¹⁶-cm⁻³ carrier concentration and 220 cm²/V s Hall mobility at 300 K.¹⁵ “As-received” samples were ultrasonically cleaned in acetone, dimethylsulfoxide, methanol, isopropyl alcohol, and de-ionized water, then nitrogen blow dried. Both Zn- and O-faces from separate halves of the same ZnO crystal were ROP processed for 2 h. Arrays of Au and Pd diodes (0.4 mm diameter, 30 nm thick) were e-beam deposited *in situ* on two ROP-cleaned and as-received polar surfaces at mid-10⁻⁹-Torr pressures. Subsequently, we e-beam deposited (40/60/30 nm) Ti/Ni/Au Ohmic contacts on the entire backside of each ZnO piece.

Figure 1 shows DRCL spectra (a) and relative defect intensity changes versus depth (b) for ROP-treated Zn and O faces. Electron beam energies E_B varied from 1 to 5 keV, corresponding to depths U_0 of peak electron-hole pair creation rates increasing from 10 to 100 nm, respectively. The 2.5 eV “green” defect (I_D) and 3.45 eV near band edge (I_{NBE}) emission intensity exhibit significant polarity-related

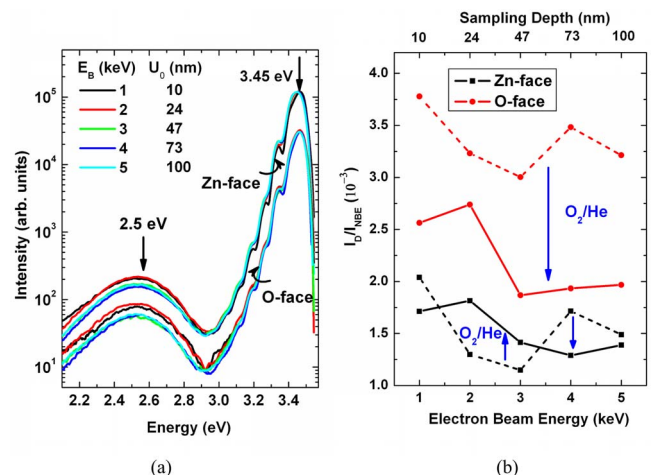


FIG. 1. (Color online) (a) DRCL spectra and (b) relative defect intensity changes vs depth for ROP-treated (0001) Zn and (000 $\bar{1}$) O faces.

^{a)} Author to whom correspondence should be addressed. Electronic mail: dong.70@osu.edu.

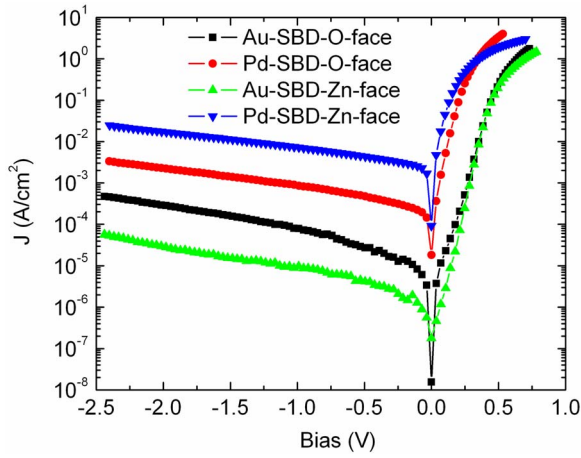


FIG. 2. (Color online) Typical I - V characteristics at 300 K for Au and Pd SBDs on ROP-treated Zn and O faces.

differences. Although spectral features appear similar, the Zn face displays four times higher NBE emission throughout the near-surface region. The O face has two times higher defect intensity than the Zn face even after ROP cleaning. As-received surfaces show similar polarity effects. Figure 1(b) shows ROP cleaning effectively decreases the O-face I_D/I_{NBE} ratio, while changing the Zn-face ratio only slightly.

The higher I_D of 2.5 eV defects, previously associated with O vacancies,^{9,10} induces different transport behavior on the O- versus Zn-face-metal diodes. First, resistivity of two Au Ohmic contacts on Zn face increases monotonically while that on O face decreases slightly as temperature decreases from 300 to 100 K (not shown here).¹⁶ This indicates more near-surface defects at the O versus the Zn face, consistent with the DRCLS results. For Au and Pd Schottky barrier diodes (SBDs) on ROP-treated surfaces, typical I - V characteristics at 300 K in Fig. 2 show a conversion from Ohmic to rectifying behavior for both metals and both polarities. Although all are rectifying, these SBDs are both metal and polarity dependent. In general, Au-/Zn-face SBDs have ten times lower leakage current and higher rectification, than Au-/O-face SBDs. Pd SBDs always have larger currents than Au SBDs in the entire bias region, with Pd on the Zn face the highest. Assuming that thermionic emission (TE) dominates forward current, then for $V > 3 kT/q$, the current is $I = I_S(\exp[q(V - IR_S)/\eta kT] - 1)$, with $I_S = AA^*T^2 \exp(-q\Phi_{SB}^{IV}/kT)$ the saturation current, R_S the series resistance, η the ideality factor, A the diode area ($1.25 \times 10^{-3} \text{ cm}^2$), A^* the effective Richardson constant ($32 \text{ A cm}^{-2} \text{ K}^{-2}$), and Φ_{SB}^{IV} the zero-biased strip buried heterostructure. Ideality factor η and effective barrier heights from a TE model are summarized in Table I and show different rectifying behaviors for Au versus Pd SBDs, notwith-

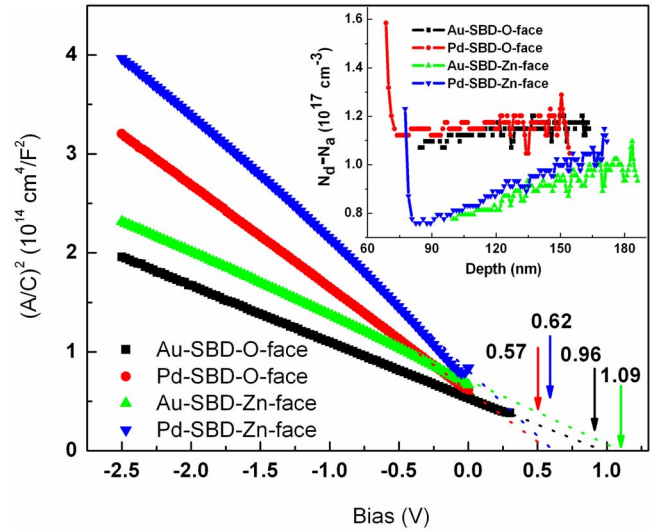


FIG. 3. (Color online) Typical $1/C^2$ - V curves at 300 K for Au- and P-SBDs on ROP-treated Zn and O faces, with associated carrier concentration profiles shown in the inset.

standing the same work function values.¹⁷ Furthermore, the very different SBD behavior for the same metal, either Au or Pd, on the Zn or O face indicates strong polarity effects. Note that TE model alone cannot account for the large reverse currents, especially for Pd SBDs, where defect-assisted tunneling and/or hopping may play a role.

Figure 3 shows the C^{-2} - V characteristics at 1 MHz and associated depth-dependent carrier concentration for the same Au and Pd SBDs, along with Φ_{SB}^{CV} values calculated from $\Phi_{SB}^{CV} = V_i + V_0 + kT/q$ with V_i the intercept and $V_0 = (kT/q) \ln(N_C/N_D)$.¹⁸ C^{-2} - V characteristics are linear only for O-face SBDs. Table I shows Φ_{SB}^{CV} values for the SBDs extracted by linear fitting. The associated carrier density profiles (Fig. 3 inset) are strongly polarity dependent. Net carrier concentrations ($N_d - N_a = N_{\text{eff}}$) are constant for both the Au and Pd SBDs on the O face in the near-surface region (90–170 nm), whereas they gradually decrease by about 30% in the same region for Au and Pd on the Zn-polar surface. Also, N_d increases sharply for the Pd SBDs on both polar surfaces at the shallowest depths profiled by C - V .

To account for these metal- and polarity-dependent carrier concentration profiles, we describe the effective donor concentration N_d^{eff} as

$$N_d^{\text{eff}} = N_d^{\text{bulk}} + N_d^{\text{surf}} \exp(-z/d_1) - N_a^{\text{surf}} \exp(-z/d_2), \quad (1)$$

where N_d^{bulk} is the bulk donor concentration, and N_d^{surf} and N_a^{surf} are surface donor and acceptor densities decaying away from the surface with decay lengths d_1 and d_2 , respectively. The sharp N_d increase for Pd SBDs near the surface may be due to hydrogen incorporation at the interface since hydro-

TABLE I. SBD characteristics at 300 K for Pd and Au on Zn- and O-polar surfaces.

Surface	Schottky metal	Ideality η	Φ_{SB}^{IV} (eV)	Φ_{SB}^{CV} (eV)	Nd-Na ($\times 10^{17} \text{ cm}^{-3}$)
(0001) Zn	Au	1.2	0.81	1.20	0.7–1.0
(0001) Zn	Pd	1.3	0.53	0.73	0.8–1.0
(000 $\bar{1}$) O	Au	1.3	0.77	1.07	1.1
(000 $\bar{1}$) O	Pd	1.2	0.61	0.68	1.1

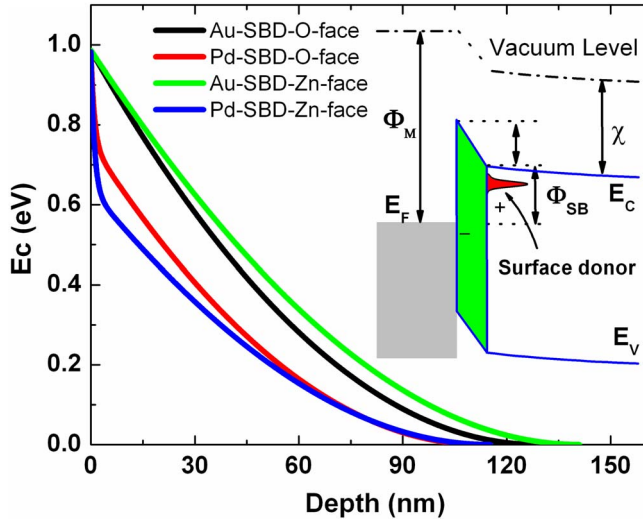


FIG. 4. (Color online) Calculated conduction band diagrams for Au and Pd SBDs on the Zn and O faces with the formation of interface dipole (ΔV) at Pd/ZnO interfaces shown in the inset.

gen easily penetrates Pd thin films. Indeed, recent low- T (80 K) photoluminescence spectra provide evidence of H indiffusion on Pd/ZnO interface in terms of an enhanced bound exciton I_4 (~ 3.36 eV) for Pd SBDs, as compared to Au SBDs, especially on the Zn face.¹⁶ This is also consistent with the most leaky I - V characteristic for Pd SBDs on the Zn face. The N_d^{surf} term describes the sharp N_d^{eff} increase within the outer few nanometers due to H and perhaps to impurity segregation from the bulk.¹⁹ DLTS of both Zn- and O-face diodes reveal two dominant traps, including the well-known bulk traps E_3 (0.27 eV) and E_4 (0.49).^{20,21} However, a surface-related trap, E_s ($< \sim 95$ nm deep, 0.49 eV) for the Pd/Zn-face SBDs, made on 1 h ROP-treated ZnO, was not observed on the SBDs in this study. Interestingly, preliminary DLTS results reveal that densities of the E_4 trap, consistent with the 2.5 eV emission, in the Au SBDs can be significantly influenced by the surface polarity, i.e., higher on the O face and lower on the Zn face. Detailed DLTS and DRCLS correlations will be published elsewhere.¹⁶

An N_d^{surf} surface acceptor term with $d_2 \sim 100$ nm accounts for the Zn-face N_d^{eff} subsurface decrease, possibly due to piezoelectric fields, plasma treatment, and/or strain that induce diffusion of charged defect or impurity segregation toward the positively charged surface. This is currently under investigation. The rapidly increasing N_d^{eff} near the Pd/ZnO (0001) and (000 $\bar{1}$) interfaces narrows the surface space charge region calculated from Poisson's equation with reasonable values assigned to the terms in Eq. (1), as shown in Fig. 4. Unlike the Au/ZnO(0001) and (000 $\bar{1}$) interfaces, the

sharp decrease of the potential at the intimate interface of Pd diodes represents a negative interface dipole (see Fig. 4 inset). Thus tunneling through a hydrogen-induced interface dipole decreases the effective Schottky barrier. In addition, introduction of N_d^{surf} widens the SBDs' depletion region on the Zn versus O face. The revised band bending is consistent with the Table I values of Φ_{SB}^{CV} and Φ_{SB}^{IV} , and accounts for the metal and polarity dependences. Overall, Zn- and O-polar ZnO surfaces and SBDs display strong electronic and optical differences that correlate with defect emissions, traps, and metal/ZnO interface chemistries.

The authors gratefully acknowledge support from the National Science Foundation Grant No. DMR-0513968 (Verne Hess), Dr. Wu Lu, and Michael Schuette for C - V measurements.

- ¹S. J. Pearton, D. P. Norton, K. Ip, Y. W. Heo, and T. Steiner, *Prog. Mater. Sci.* **50**, 293 (2005).
- ²B. J. Coppa, R. F. Davis, and R. J. Nemanich, *Appl. Phys. Lett.* **82**, 400 (2003).
- ³H. L. Mosbacker, Y. M. Strzhemechny, B. D. White, P. E. Smith, D. C. Look, D. C. Reynolds, C. W. Litton, and L. J. Brillson, *Appl. Phys. Lett.* **87**, 012102 (2005).
- ⁴M. W. Allen, M. M. Alkaiji, and S. M. Durbin, *Appl. Phys. Lett.* **89**, 103520 (2006).
- ⁵M. W. Allen and S. M. Durbin, *Appl. Phys. Lett.* **92**, 122110 (2008).
- ⁶R. Schifano, E. V. Monakhov, U. Grossner, and B. G. Svensson, *Appl. Phys. Lett.* **91**, 193507 (2007).
- ⁷Q. L. Gu, C. K. Cheung, C. C. Ling, A. M. C. Ng, A. B. Djursic, L. W. Lu, X. D. Chen, S. Fung, C. D. Beling, and H. C. Ong, *J. Appl. Phys.* **103**, 093706 (2008).
- ⁸K. Ip, G. T. Thaler, H. Yang, S. Y. Han, Y. Li, D. P. Norton, S. J. Pearton, S. Jang, and F. Ren, *J. Cryst. Growth* **287**, 149 (2006).
- ⁹L. J. Brillson, H. L. Mosbacker, M. J. Hetzer, Y. Strzhemechny, G. H. Jessen, D. C. Look, G. Cantwell, J. Zhang, and J. J. Song, *Appl. Phys. Lett.* **90**, 102116 (2007).
- ¹⁰H. L. Mosbacker, C. Zgrabik, M. J. Hetzer, A. Swain, D. C. Look, G. Cantwell, J. Zhang, J. J. Song, and L. J. Brillson, *Appl. Phys. Lett.* **91**, 072102 (2007).
- ¹¹C. Wöll, *Prog. Surf. Sci.* **82**, 55 (2007).
- ¹²M. W. Allen, P. Miller, R. J. Reeves, and S. M. Durbin, *Appl. Phys. Lett.* **90**, 062104 (2007).
- ¹³S. A. Chevtchenko, J. C. Moore, Ü. Özgür, X. Gu, A. A. Baski, H. Morkoç, B. Nemeth, and J. E. Nause, *Appl. Phys. Lett.* **89**, 182111 (2006).
- ¹⁴D. C. Look and Z.-Q. Fang, *Appl. Phys. Lett.* **79**, 84 (2001).
- ¹⁵D. C. Look, *Zinc Oxide and Related Materials*, MRS Symposia Proceedings No. 957 (Materials Research Society, Pittsburgh, 2007), p. 127.
- ¹⁶Z.-Q. Fang, Y. F. Dong, D. C. Look, and L. J. Brillson (unpublished).
- ¹⁷H. B. Michaelson, *J. Appl. Phys.* **48**, 4729 (1977).
- ¹⁸D. K. Schroder, *Semiconductor Material and Device Characterization* (Wiley, New York, 1998).
- ¹⁹D. C. Look, B. Claffin, and H. E. Smith, *Appl. Phys. Lett.* **92**, 122108 (2008).
- ²⁰Z.-Q. Fang, B. Claffin, D. C. Look, Y. F. Dong, H. L. Mosbacker, and L. J. Brillson, "Surface traps in vapor-phase-grown bulk ZnO studied by deep level transient spectroscopy", *J. Appl. Phys.* (to be published).
- ²¹F. D. Auret, S. A. Goodman, M. J. Legodi, W. E. Meyer, and D. C. Look, *Appl. Phys. Lett.* **80**, 1340 (2002).